

A Novel Miniaturized Capacitor Loaded Interdigital Filter

Luyao Tang*, Xiaoli Jiang, Hao Wei, Weiwei Liu, and Wei Han

Abstract—This paper proposes a novel miniaturized interdigital capacitor loaded interdigital filter, which is applied in C-band (3.2 GHz \sim 4.2 GHz). By loading an interdigital capacitor on the open end of the resonator of the interdigital filter, the length of the resonator is shortened by 28%. The resonant frequency offset caused by tap introduction is adjusted by using the method of impedance compensation at the open end of resonator 1 and resonator 5, which further reduces the size of the filter. The miniaturized filter is fabricated on a 0.254 mm-thickness alumina substrate with relative dielectric constant of 9.8 by thin film process. Measured results are as follows: the passband of the filter is 3.2 GHz \sim 4.2 GHz; the insertion at center frequency is -1 dB; the return loss is less than -18.3 dB. The size of the filter is 4.98 mm \times 6.45 mm ($0.15\lambda_g \times 0.20\lambda_g$), which is 37.8% smaller than that of the traditional interdigital filter.

1. INTRODUCTION

As a frequency selective device for separating signals from different frequencies, filters are widely used in various communication systems [1, 2]. In recent years, the demand for filters in communication systems is developing towards miniaturization and low cost [3, 4]. New processes and novel structures have been adopted to reduce the size of filters. In [5], combined with low temperature co-fired ceramic (LTCC) process, an interdigital filter with center frequency of 6.5 GHz is designed, and its size is only 5 mm \times 6 mm \times 0.4 mm. In [6], a filter with a center frequency of 4.1 GHz is designed with the advantage of multi-layer design of micro-electro-mechanical systems (MEMS) process, and its size is only 7 mm \times 7.8 mm \times 0.8 mm. In [7], a miniaturized filter is designed through stepped-impedance resonator (SIR) and defected ground structure (DGS), which is 38% smaller than the conventional hairpin filter. In [8], a compact high-performance filter is designed through cross coupling. Its size is only 7.2 mm \times 8 mm ($0.21\lambda_g \times 0.24\lambda_g$), and the out-of-band rejection reaches -60 dBc.

Because of its compact structure, interdigital filter is often used in the miniaturization design of filter [9]. Many researchers have designed miniaturized interdigital filters through various methods. In [10], a miniaturized interdigital filter is designed through broadside coupling based on LTCC. Its center frequency is 3 GHz, and its size is only 6 mm \times 10 mm. In [11], a two-layer interdigital filter is designed based on MEMS process, and its size is only 7 mm \times 3 mm \times 0.8 mm. Although LTCC and MEMS processes can achieve small size through multi-layer design, they are more expensive than PCB or thin film processes. In [12], an interdigital filter with an L-shaped structure composed of a SIR is designed based on thin film process. Its size is only 5 mm \times 5 mm ($0.35\lambda_g \times 0.35\lambda_g$). Although the size of the resonator can be shortened by SIR, it can be reduced by further extent.

In this paper, a miniaturized interdigital filter based on thin film process is designed, simulated, fabricated, and measured. By loading interdigital capacitor on the open end of the resonator, the size of the resonator is reduced by 28%. Then the size of the filter is further reduced by impedance

Received 12 January 2022, Accepted 7 March 2022, Scheduled 18 March 2022

* Corresponding author: Luyao Tang (tangluyao613@163.com).

The authors are with The 54th Research Institute of China Electronics Technology Group Corporation (CETC-54), Shijiazhuang 050051, China.

compensation. The size of the miniaturized interdigital filter is $4.98 \text{ mm} * 6.45 \text{ mm}$ ($0.15\lambda_g * 0.20\lambda_g$), which is 37.8% smaller than that of the traditional interdigital filter. The filter is processed on a 0.254 mm-thickness Alumina ceramic substrate, and the S parameters of the filter is measured. The measured results of the filter are corresponding to the simulation ones.

2. DESIGN AND SIMULATION OF THE INTERDIGITAL FILTER

In order to show the miniaturization effect of capacitor loaded interdigital filter, a 5th order Chebyshev type conventional interdigital filter with passband from 3.2 GHz to 4.2 GHz is designed and compared with capacitor loaded interdigital filter. They are processed by thin film process on a 0.254 mm-thickness Alumina ceramic substrate which has a loss tangent $\tan \delta$ of 0.002 and relative dielectric constant ϵ_r of 9.8.

2.1. Design Method of Conventional Interdigital Filter

The structure of a tap fed interdigital filter is shown in Fig. 1. The design of a tap fed interdigital filter is divided into three steps [13]: 1. Determining the resonator size according to the center frequency of the filter to be designed, 2. Determining the spacing between resonators according to the coupling coefficient, 3. Determining the tap position according to the relationship between the external quality factor Q_e and the tap position.

The length of the interdigital filter resonator is one fourth of the wavelength of the center frequency f_0 on the dielectric substrate. By using HFSS software to fine tune the resonator, the length of resonator $L = 7.78 \text{ mm}$ at $f_0 = 3.67 \text{ GHz}$ is obtained. Taking the spacing S between the two resonators as a variable, the coupling coefficient between the two resonators is simulated, and the relationship curve between the coupling coefficient and the spacing is obtained. The size of individual resonator and the coupling between resonators are shown in Fig. 2.

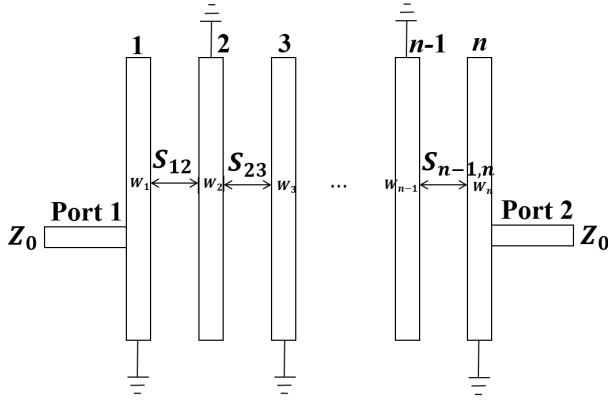


Figure 1. Structure diagram of conventional interdigital filter.

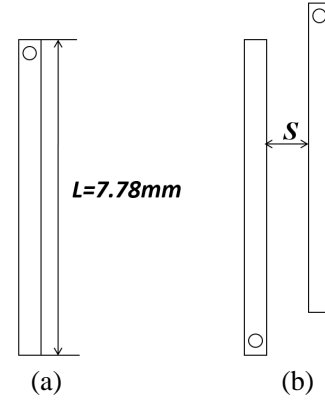


Figure 2. Resonator and coupling between resonators.

The coupling coefficient is simulated by the eigenmode of HFSS software. The simulation formula of coupling coefficient is as follows:

$$k = \frac{f_2^2 - f_1^2}{f_1^2 + f_2^2} \quad (1)$$

where f_1 and f_2 are the first and second eigenmode frequencies of the coupled resonator. The relationship curve between the coupling coefficient and the spacing of each resonator is shown in Fig. 3. Considering the general engineering application requirements, a 5th order Chebyshev filter with ripple coefficient ϵ of 0.04321 dB will be designed. The low-pass prototype parameters of the filter are $g_0 = g_6 = 1$, $g_1 = g_5 = 0.9714$, $g_2 = g_4 = 1.3721$, and $g_3 = 1.8014$. The theoretical calculation formula of coupling

coefficient of the filter to be designed is as follows:

$$k_{ij} = \frac{FBW}{\sqrt{g_i * g_j}} \quad (2)$$

where k_{ij} is the theoretically required coupling coefficient between resonator i and resonator j , and FBW is the fractional bandwidth of the filter. The coupling coefficient between the resonators is $k_{12} = k_{45} = 0.2601$, $k_{23} = k_{34} = 0.1912$. The calculated coupling coefficient is compared with the simulation coupling curve, and then coupling spacing S_{ij} is obtained, where S_{ij} is the spacing between resonators i and j , $S_{12} = S_{45} = 0.13$ mm, $S_{23} = S_{34} = 0.2$ mm.

The position of the input and output of the filter affects the external quality factor Q_e . The calculation formula of the external Q_e is as follows:

$$Q_e = \frac{g_0 g_1}{FBW} \quad (3)$$

The tap position is decided by the group delay of S_{11} and Q_e . The relationship between the group delay of S_{11} and the external quality factor Q_e is as follows [14]:

$$\tau_{s_{11}}(f_0) = \frac{2Q_e}{\pi f_0} \quad (4)$$

According to the above formula, we can get $\tau_{s_{11}}(f_0) = 562$ ps. Taking the feeding position t as a variable, the group delay is simulated, and the values of the group delay at different t values are obtained. We adjust the feed position so that the group delay at its center frequency is 562 ps, and t is equal to 3 mm. The simulation results are shown in Fig. 4.

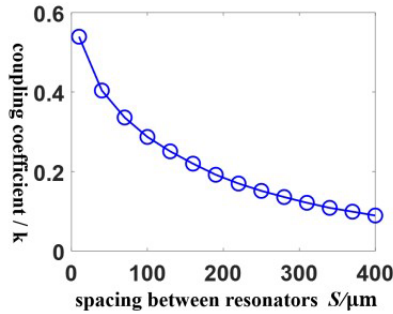


Figure 3. Relationship curve of the coupling coefficient and spacing between resonators.

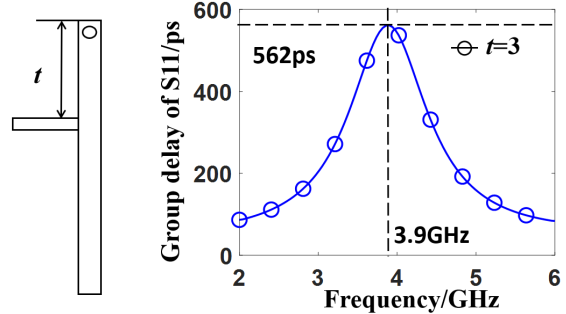


Figure 4. Tap position and group delay curve of S_{11} .

As seen from Fig. 4, the tap affects the resonant frequency of the resonator, and move the resonant frequency of the resonator from 3.67 GHz to 3.9 GHz. It is necessary to increase the length of the resonator to correct the resonant frequency. We increase the length of the resonator by $AL = 0.38$ mm so that its resonant frequency is 3.67 GHz. After increasing the resonator length and moving the resonant frequency to 3.67 GHz, the group delay of S_{11} also changes. We simulate the group delay of the filter again and get the curve of the group delay with the different tap positions as shown in Fig. 5. When t is equal to 3.15 mm, the group delay meets the design requirements. The structure and size of the 5th order interdigital filter are shown in Fig. 6.

The simulation results of the filter are shown in Fig. 7. The passband of the filter is 3.2 GHz \sim 4.2 GHz; the maximum insertion loss in the passband is 0.25 dB; and the rejection at 2.2 GHz and 5.2 GHz are -34.7 dBc and -58.7 dBc respectively.

2.2. Design of Interdigital Capacitor Loaded Interdigital Filter

The method of loading capacitance at the open end of interdigital resonator is often used to reduce the length of resonator [15, 16]. However, the design of miniaturized filters using capacitor loading is often

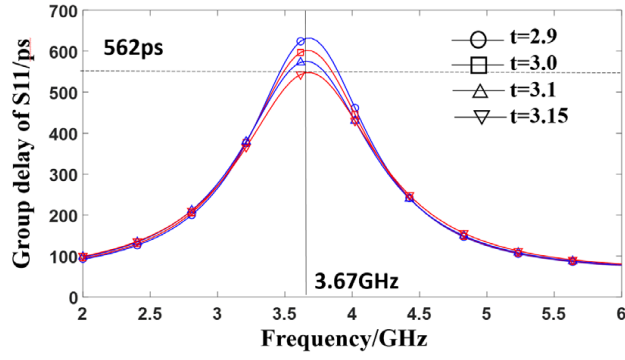


Figure 5. Group delay curves under different variables t .

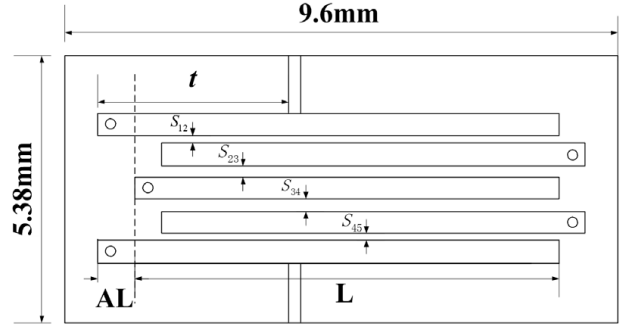


Figure 6. 5th order interdigital filter.

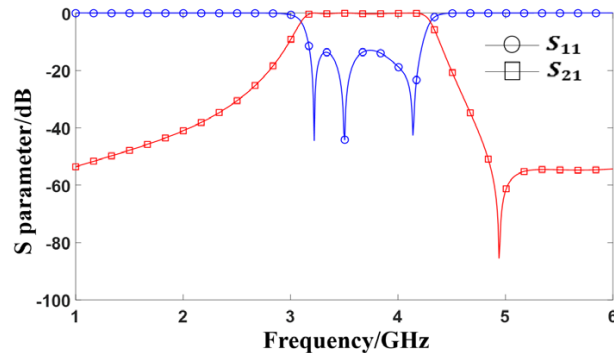


Figure 7. Simulation results of 5th order interdigital filter.

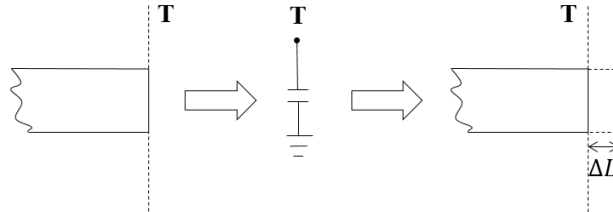


Figure 8. Equivalent model of open end of microstrip line.

used in filters fabricated by 3D processed such LTCC or MEMS. Filters designed by LTCC process or MEMS process often use the multi-layer design of the process to construct metal-insulator-metal (MIM) capacitors to achieve a large enough capacitance. At present, LTCC and MEMS filters have higher price and lower yield than 2D filters designed by thin film process. The main content of this paper is how to miniaturize the filter by capacitor loading based on 2D thin film process.

The influence of the loading capacitor on the length of the resonator is quantitatively analyzed by the length extension model of the capacitor at the open end of the microstrip line to the line length. The equivalent model of the open end of the microstrip line is shown in Fig. 8. At the open end of a microstrip line, the field propagation will not stop suddenly due to the influence of the fringe field, but will slightly extend the distance from one end. This effect can be equivalent by equivalent parallel capacitor, and the relationship between the extension length Δl and various parameters is as follows [14]:

$$\Delta l = \frac{cZ_c C_p}{\sqrt{\epsilon_{re}}} \quad (5)$$

where c is the speed of light in free space, C_p the capacitance of equivalent loading capacitor, Z_c the

characteristic impedance of microstrip line, and ϵ_{re} the equivalent relative dielectric constant.

According to the above analysis, how to introduce enough capacitance at the open end of the interdigital resonator is a key factor to the filter miniaturization. According to the equivalent capacitance extraction formula [17], the capacitance value can be extracted in HFSS software.

$$C = -\frac{1}{2\pi f \text{Im}(Z_{11})} \tag{6}$$

For planar filter design, the most common capacitor is slot capacitor. However, slot capacitance cannot be used to achieve large capacitance. The slot capacitor with a width of 0.4 mm and a gap of 0.05 mm is simulated, and the capacitance value of the slot capacitor is obtained, as show in Fig. 9(a).

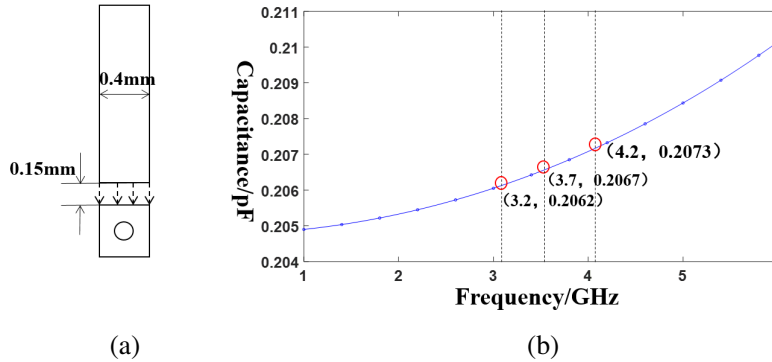


Figure 9. Slot capacitor and capacitance extraction.

It can be known that the slot capacitance is only 0.207 pF at the center frequency. Substituting $Z_c = 38.3$, $\sqrt{\epsilon_{re}} = 2.67$ into formula (5), the length that the slot capacitor can extend is $\Delta l = 0.88$ mm. Due to the loaded capacitor, the length of the resonator is increased by 0.45 mm. The overall size of the resonator is only reduced by 0.33 mm (0.88 mm–0.45 mm), which is almost negligible for the quarter wavelength at 3.67 GHz which is 7.78 mm.

The interdigital capacitors are distributed through the interdigital fingers of multi-section microstrip lines to form a plurality of parallel capacitors to realize larger capacitance. The structural model of interdigital capacitor is shown in Fig. 10(a). Using HFSS software to extract the capacitance of the interdigital capacitor, the results are shown in Fig. 10(b).

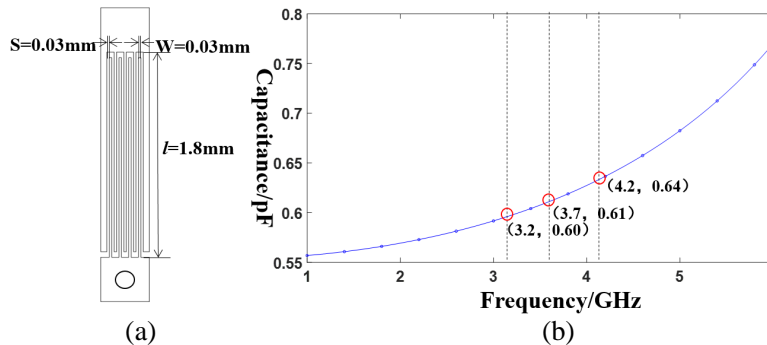


Figure 10. Capacitance extraction of interdigital capacitor.

The capacitance of interdigital capacitor extracted by software at 3.7 GHz is 0.61 pF. Substituting into formula (5), the shortened length of the resonator loaded with the interdigital capacitor is $\Delta l = 2.63$ mm. The length of the loaded interdigital capacitor is increased by 0.45 mm, and the overall length of the resonator is reduced by 2.18 mm, which is 28% for the resonator with a quarter wavelength of 7.78 mm.

We fine tune the resonator loaded with interdigital capacitor to obtain the dimensions of the traditional resonator with center frequency of 3.67 GHz, and the resonator loaded with interdigital capacitor is as shown in Fig. 11.

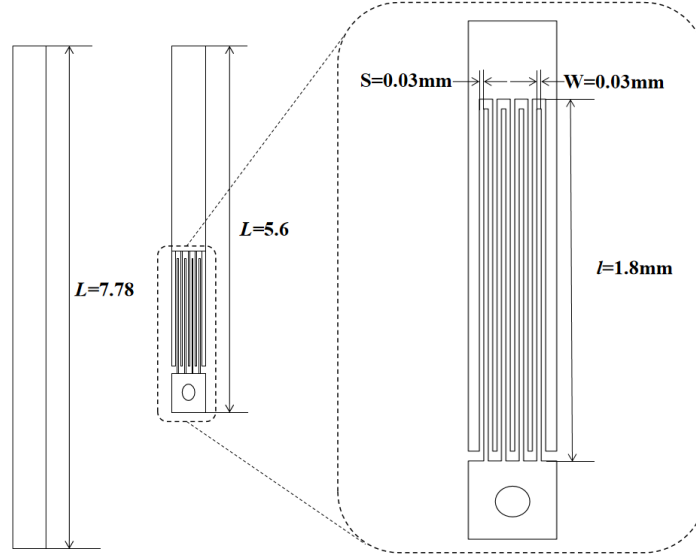


Figure 11. Conventional resonator and resonator loaded with interdigital capacitor.

The capacitor loaded interdigital filter is designed according to the design method of interdigital filter above, and the relationship curve between coupling coefficient and resonator spacing is obtained, as shown in Fig. 12.

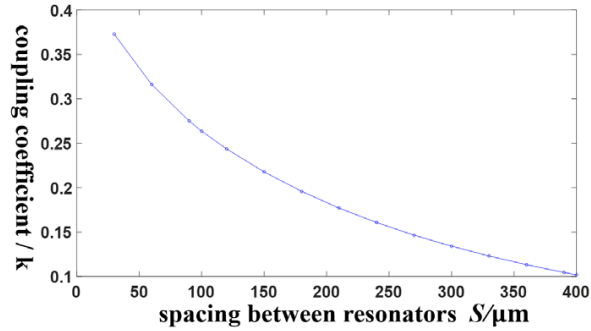


Figure 12. Relationship between coupling coefficient and spacing of loaded interdigital capacitor resonators.

The tap position is determined by the group delay. When t is equal to 3.2 mm, the group delay meets the filter design requirements, and the group delay curve is shown in Fig. 13. The resonant frequency of the resonator becomes 3.8 GHz after adding the tap. According to the above filter design method, it is necessary to increase the length of the resonator to adjust the resonant frequency to 3.67 GHz, but this will increase the size of the filter. Actually, if we do not increase the length of resonator 1 and resonator 5, the passband return loss of the filter will deteriorate.

The structure of the filter is shown in Fig. 14, where $t = 3.2$ mm, $L = 5.6$ mm, $l = 1.85$ mm, $S_{12} = S_{45} = 0.1$ mm, $S_{23} = S_{34} = 0.19$ mm. We simulate the filter without increasing the length of resonator 1 and resonator 5, and the simulation results are shown in Fig. 15.

As seen from Fig. 15, if the lengths of resonator 1 and resonator 5 are not increased, the passband return loss of the filter is poor. The simulation results show that the maximum return loss in the

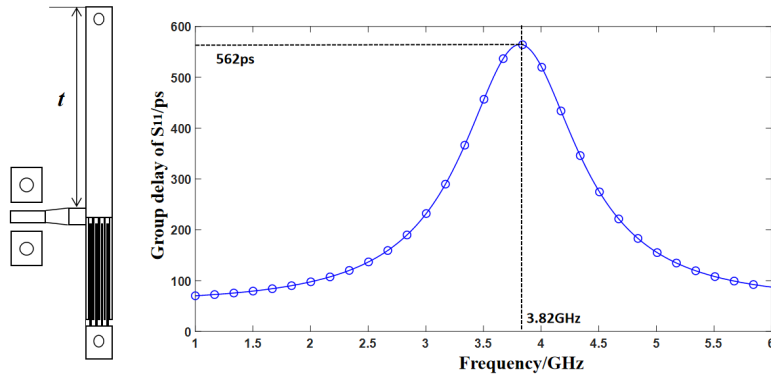


Figure 13. Group delay of interdigital capacitor loaded interdigital filter.

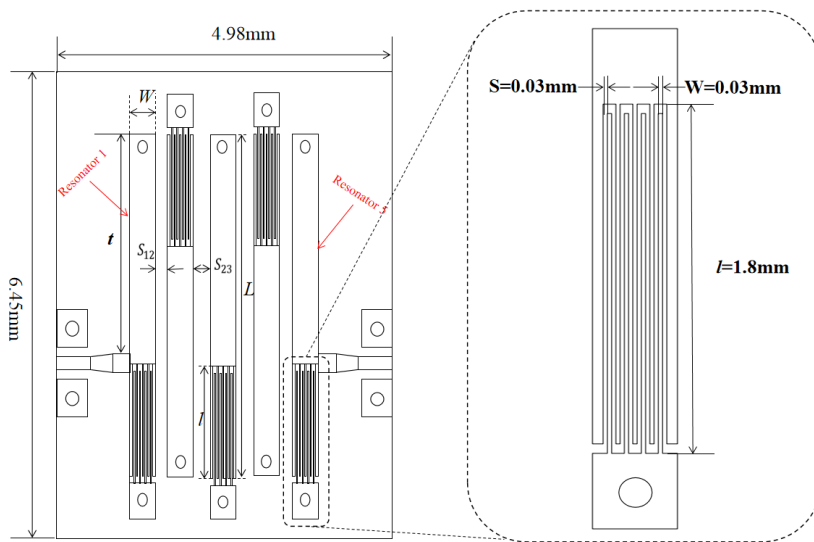


Figure 14. Interdigital capacitor loaded interdigital filter structure before adjustment.

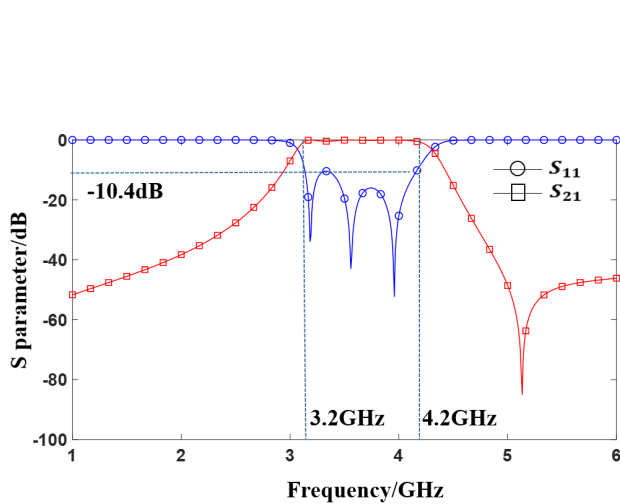


Figure 15. Simulation results of miniaturized filter without adjustment.

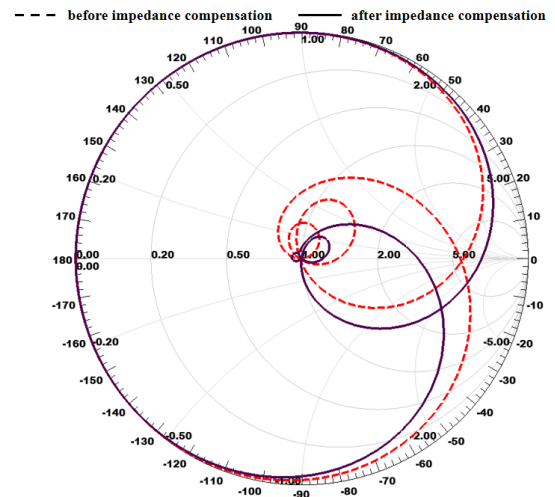


Figure 16. Smith impedance circle diagram of the filter.

passband is -10.4 dB. After processing, the return loss in the filter band will further deteriorate and need to be improved. The Smith impedance circle diagram of the filter before adjustment is shown by the dotted line in Fig. 16. The impedance of the filter is inductive as a whole, so it needs impedance compensation to optimize the return loss in the passband.

The method of impedance compensation on resonator 1 and resonator 5 is used to increase the overall capacitance of the filter to optimize the passband return loss of the filter. The structure of the filter after impedance compensation is shown in Fig. 17. In HFSS, we optimize the target of return loss less than -17 dB, and get $k_1 = 1.5$ mm, $k_2 = 0.15$ mm.

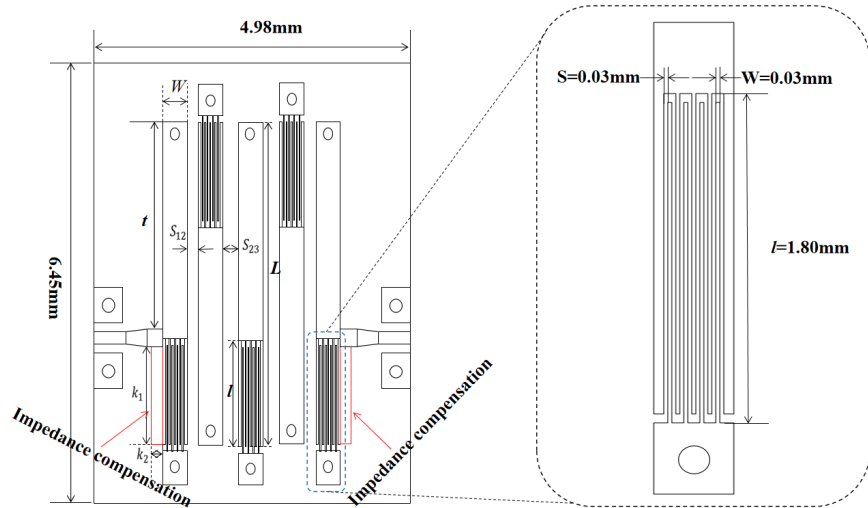


Figure 17. Interdigital capacitor loaded interdigital filter structure.

The simulation results of the interdigital capacitor loaded interdigital filter are shown in Fig. 18. The passband of the filter is 3.2 GHz \sim 4.25 GHz; the maximum insertion loss in the passband is 0.12 dB; the maximum return loss in the passband is -17.3 dB; and the rejections at 2.2 GHz and 5.2 GHz are -34.8 dBc and -77 dBc, respectively. The size of filter is 4.98 mm \times 6.45 mm.

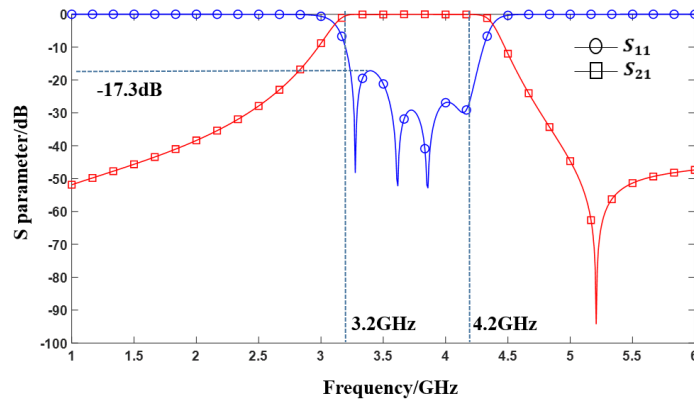


Figure 18. Simulation results of interdigital capacitor loaded interdigital filter.

3. MEASUREMENT AND COMPARISON

The filter is fabricated by the thin film process, and the filter photo is shown in Fig. 19. The filter is measured with probe station and vector network analyzer. The insertion loss, return loss in passband,

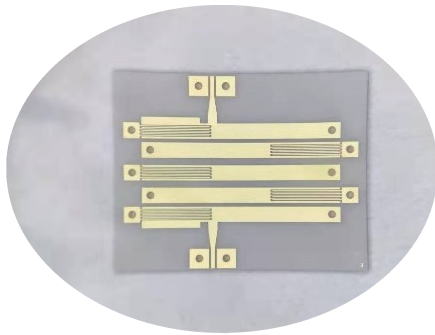


Figure 19. Physical drawing of miniaturized interdigital filter.

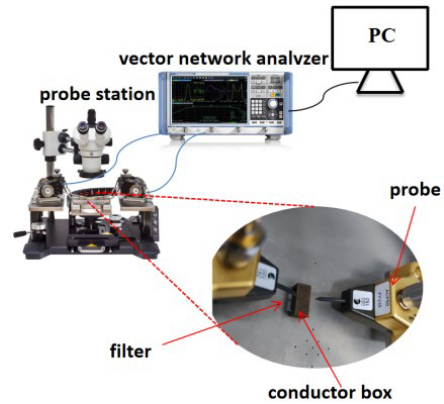


Figure 20. Measurement system.

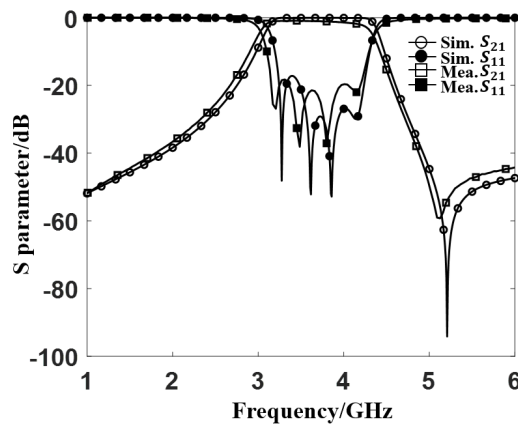


Figure 21. Comparison between simulated and measured results of filter.

Table 1. Comparison with published BPFs.

Reference	Process	f_0 (GHz)	FBW (%)	RL (dB)	IL (dB)	Suppression	Size ($\lambda_g * \lambda_g$)
[5]	LTCC	6.5	30.7	≤ -15	2	-40 dBc@11.6 GHz	0.26 * 0.32
[6]	MEMS	4.1	15.0	≤ -14	4	-45 dBc@5 GHz	0.32 * 0.35
[8]	Thin Film	3.7	27	≤ -15	2	-60 dBc@4.8 GHz	0.21 * 0.24
[12]	Thin Film	8.0	15.0	≤ -20	2.5	-45 dBc@9.5 GHz	0.35 * 0.35
[18]	PCB	10.2	18.2	≤ -18	1.5	-50 dBc@12.2 GHz	0.79 * 1.33
[19]	PCB	2.0	15.0	≤ -10	1.1	NA	0.35 * 0.4
This work	Thin Film	3.7	27	≤ -18	1	-55 dBc@5.2 GHz	0.15 * 0.2

and the rejection out of band of the filter are obtained by using the measurement system in Fig. 20.

The comparison between the simulated and measured S parameters of the filter is shown in Fig. 21, and the simulation results agree with the measured ones. The measured passband of the filter is 3.2 GHz \sim 4.2 GHz; the insertion at center frequency is -1 dB; the return loss is less than -18.3 dB; and the rejections at 2.2 GHz and 5.2 GHz are -33 dBc and -54.6 dBc, respectively.

In Table 1, the capacitor loaded miniaturized filter proposed in this paper is compared with other published filters. The filter proposed by this work has smaller size and lower insertion loss, and the size of the filter is even smaller than the LTCC and MEMS based filters.

4. CONCLUSION

Miniaturization and low cost are the developing trends of filters. The planar microstrip filter based on thin film process can meet the demands of both miniaturization and low cost. In this paper, a novel interdigital capacitor loaded miniaturized interdigital filter is designed, simulated, fabricated, measured, and compared. By loading an interdigital capacitor, the size of the miniaturized interdigital filter is $4.98 \text{ mm} * 6.45 \text{ mm}$ ($0.15\lambda_g * 0.20\lambda_g$), which is 37.8% smaller than that of the traditional interdigital filter. The filter is measured with a probe station, and the measured results are corresponding with the simulated ones. Compared with other planar microstrip filters, the filter designed in this paper has smaller size and lower insertion loss.

REFERENCES

1. Aiswarya, S., S. Bhuvana Nair, L. Meenu, and S. K. Menon, "Analysis and design of stub loaded closed loop microstrip line filter for Wi-Fi applications," *2019 Sixteenth International Conference on Wireless and Optical Communication Networks (WOCN)*, 1–5, 2019.
2. Haddi, S. B., A. Zugari, A. Zakriti, and S. Achraou, "A compact microstrip T-shaped resonator band pass filter for 5G applications," *2020 International Conference on Intelligent Systems and Computer Vision (ISCV)*, 1–5, 2020.
3. Luo, L., H. Tie, Q. Ma, and B. Zhou, "Compact LTCC filter with 7th-order harmonics suppression for 5G N77 band applications," *Progress In Electromagnetics Research Letters*, Vol. 98, 69–74, 2021.
4. Wang, P., K. Duan, M. Li, M. Zhang, and B. Jin, "A novel miniaturized L-band filter with great stopband characteristics using interdigitated coupled lines CRLH-TL structure," *Progress In Electromagnetics Research C*, Vol. 114, 57–67, 2021.
5. Cheng, T., W. Yang, and Y. Ze, "Development of C-band embedded layout filter based on LTCC," *Electronic Design Engineering*, Vol. 28, No. 19, 107–112, 2020.
6. Peng, Y., B. Jia, X. Yang, et al., "Design of C-band double-layer MEMS filter," *Journal of Microwave*, No. S1, 223–226, 2016.
7. Zhang, M., M. Li, P. J. Zhang, K. Duan, B. Jin, L. Huang, and Y. Song, "A novel miniaturized bandpass filter basing on stepped-impedance resonator," *Progress In Electromagnetics Research Letters*, Vol. 97, 77–85, 2021.
8. Tang, L., X. Jiang, H. Wei, and W. Liu, "A novel miniaturized C-band bandpass filter," *Progress In Electromagnetics Research M*, Vol. 106, 167–177, 2021.
9. Bharathi, R. D., J. E. Yamini, A. Evangeline, and D. B. Narayanan, "Design and analysis of interdigital microstrip bandpass filter for center frequency 2.4 GHz," *2017 Third International Conference on Science Technology Engineering & Management (ICONSTEM)*, 930–933, 2017.
10. Li, H., "Design and realization of a microminiaturized filter based on broadside-coupled interdigital structure," *2012 International Conference on Microwave and Millimeter Wave Technology (ICMMT)*, 1–3, IEEE, 2012.
11. Zhang, X., Q. Zhai, Z. Li, W. Ou, and Y. Ou, "Design of a K-band two-layer microstrip interdigital filter exploiting aggressive space mapping," *Journal of Electromagnetic Waves and Applications*, Vol. 32, No. 17, 2281–2291, 2018.
12. Min, T., X. Yang, M. Yong, et al., "Design of C-band interdigital filter and compact C-band hairpin bandpass film filter on thin film substrate," Springer International Publishing, 2017.
13. Wen, S. W., G. Yang, and X. X. Qian, "Initial design flow of tapped microstrip interdigital filter," *High Power Laser and Particle Beams*, Vol. 26, No. 09, 2262–2269, 2018.

14. Hong, J. S., *Microstrip Filters for RF/Microwave Applications*, John Wiley & Sons, USA, 2004.
15. Qiao, D. and Y. Dai, "Research on LTCC bandpass filter loaded with high performance capacitor," *Electronic Components and Materials*, Vol. 34, No. 12, 68–71, 2015.
16. Huang, X., L. Li, W. Feng, et al., "A capacitive loaded broadband waveguide filter," *Radar and Countermeasure*, Vol. 41, No. 01, 62–64, 2021.
17. Fang, J., Z. Zhuang, and Y. Dai, "Miniaturized ultra-wideband high-pass filter based on LTCC," *Research and Progress of Solid-state Electronics*, Vol. 39, No. 04, 269–272+296, 2019.
18. Xu, H. and W. Sheng, "The X-band microstrip filter design," *2017 7th IEEE International Symposium on Microwave, Antenna, Propagation, and EMC Technologies (MAPE)*, 351–355, 2017.
19. Duan, K., P. Zhang, D. Cheng, Y. Song, L. Huang, and M. Li, "Design of new miniaturized broadband bandpass filter based on SIR," *2019 Photonics & Electromagnetics Research Symposium — Fall (PIERS — Fall)*, 1640–1644, Xiamen, China, Dec. 17–20, 2019.